

Through-pellicle defect inspection of EUV masks using an ArF-based inspection tool

Dario L. Goldfarb^{*1}, William Broadbent², Mark Wylie², Nelson Felix³ and Daniel Corliss³

¹ IBM Watson Research Center, 1101 Kitchawan Rd, Yorktown Heights, NY 10598

² KLA-Tencor Corporation, One Technology Dr, Milpitas, CA 95035

³ IBM Research - Albany Nanotech, 257 Fuller Rd, Albany, NY 12203

ABSTRACT

The use of EUV photomasks in a semiconductor manufacturing environment requires their periodic inspection to ensure they are continually free of defects that could impact device yield. Defects typically occur from fall-on particles or from surface degradation such as “haze”. The proposed use of a polycrystalline-based EUV pellicle to prevent fall-on particles would preclude periodic through-pellicle mask defect inspection using e-beam, as well as, DUV inspection tools (the pellicle is opaque at DUV wavelengths). Thus, to use these types of defect inspection tools would require removal of the EUV pellicle before inspection. After inspection, the pellicle would need to be re-attached and the mask re-qualified using a test wafer, thus causing expense and delays. While EUV-wavelength inspection tools could inspect through such a pellicle precluding the need to remove the pellicle, these tools are not likely to be available in the commercial marketplace for many years. An alternate EUV pellicle material has been developed that is semi-transparent to 193nm wavelengths, thus allowing through-pellicle inspection using existing ArF-based, or other 193nm wavelength mask inspection tools. This eliminates the requirement to remove the pellicle for defect inspection and the associated time and expense. In this work, we will conduct an initial evaluation of through-pellicle EUV mask defect inspection using an existing 193nm mask inspection tool. This initial evaluation will include durability of the pellicle to defect inspection, and impact of the pellicle on inspection tool performance.

Keywords: EUV pellicle, defect inspection, metrology, EUV mask infrastructure

1. INTRODUCTION

At IBM Research, we have been working on a novel silicon-nitride EUV pellicle for some time now and have reported our recent progress [1]. This paper reports on some initial work with KLA-Tencor to investigate mask inspection tool performance when inspecting patterned EUV reticles through this pellicle. We will provide a brief background on this novel pellicle, a brief background on mask defect inspection, and the results of this initial inspection work. Finally, we will discuss our conclusions and possible future work to further characterize and possibly improve inspection through this pellicle.

2. MOTIVATION

Regular defect inspection of photomasks in a wafer fab is standard practice to prevent yield-killing repeating defects. These defects can come from fall-on particles, surface degradation such as haze, or other mechanisms. For optical masks, 193nm wavelength inspection tools are widely used in advanced wafer fabs to find very small defects. This provides effective early warning to mask degradation so the mask can be cleaned before the defects impact wafer yield. Since these optical mask pellicles are transparent at 193nm wavelength, the inspection can be quickly done with the pellicle in-place and the mask returned to use.

However, EUV masks cannot be inspected through the current polycrystalline-based pellicle because there are no commercial EUV wavelength inspection tools available yet. Further, since the pellicle is opaque to 193nm wavelength, the existing 193nm wavelength mask defect inspection tools cannot be used. This means the polycrystalline pellicle must be removed to use existing 193nm defect inspection tools (while there are also e-beam inspection tools, any pellicle must be removed). Removal and replacement of the pellicle in the wafer fab is time consuming, expensive, and allows further

*goldfarb@ibm.us.com; phone: 1-914-945-1308

contamination of the mask which then requires re-qualification using a test wafer and wafer inspection (adding more time and expense).

As we have reported previously, we have developed a novel silicon-nitride EUV pellicle which is semi-transparent at 193nm wavelength, thus allowing the use of existing 193nm wavelength defect inspection tools to inspect through the pellicle. The goal of this work is to explore 193nm wavelength inspection of EUV reticles through this pellicle assessing durability of the pellicle to inspection, the impact of the pellicle to defect sensitivity, and the impact to inspection throughput.

3. SILICON NITRIDE EUV PELLICLE

The novel silicon-nitride EUV pellicle that we have developed currently has a thickness of 19.6nm. The EUV transmission is about 87% which is similar to the current polycrystalline pellicle; we are investigating further improvements to increase EUV transmission. At 193nm wavelength, the transmission is about 38%. We have developed a fabrication process that results in a full size wrinkle-free pellicle as displayed in the photo in Figure 1.

The current pellicle design has limited heat dissipative properties in vacuum, so, at this point there is a limit to the EUV power it can withstand without wrinkling. We are working on an improved design with better heat dissipative properties which should allow higher EUV power to maintain pace with the EUV scanners.

With the defect inspection work we are reporting in this paper, we will show that initial through-pellicle inspection has now been demonstrated.

3.1 EUV pellicle 193nm transmission

The graph in Figure 2 shows the 193nm wavelength transmissive and reflective properties of the pellicle by incident angle and polarization. The solid blue line shows reasonable transmission for p-polarized light out to an incident angle of about 70 degrees – the dotted blue line is for s-polarized light. After consultation with KLA-Tencor, we both agreed this characteristic is suitable for high-resolution defect inspection and decided to proceed with initial testing. The reflected light properties are also shown.

3.2 193nm high-NA light collection

The 193nm wavelength defect inspection tool images the surface of the EUV mask using high-NA optics and an imaging sensor; it then analyzes the images to detect defects. The quality of the images ultimately determines the performance of the inspection tool; therefore, any degradation in image quality caused by the pellicle can adversely affect performance.

The diagrams in Figure 3 show the approximate 193nm wavelength light loss when inspecting through the EUV pellicle with a 193nm defect inspection tool. The left diagram shows two passes through the pellicle along with reflection from the multi-layer; this results in 10% of the incident light available to the inspection tool imaging sensor. The right diagram shows the absorber case with 2% of the incident light available to the inspection tool imaging sensor.

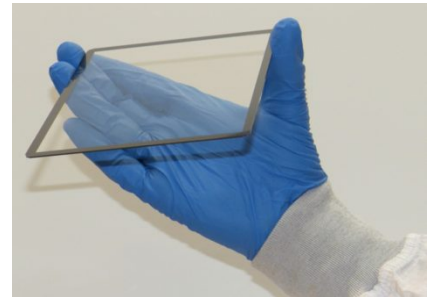


Figure 1: Full-size silicon nitride pellicle

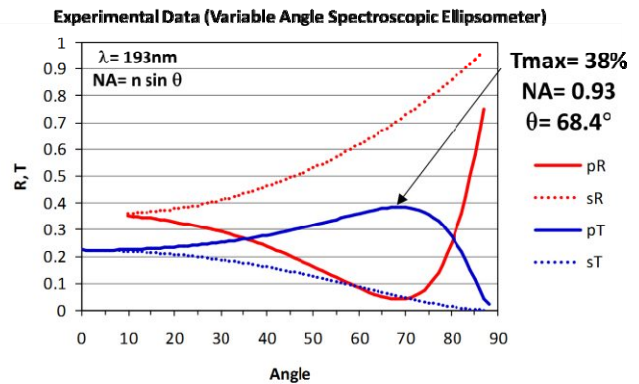


Figure 2: Pellicle transmission and reflection at $\lambda = 193\text{nm}$

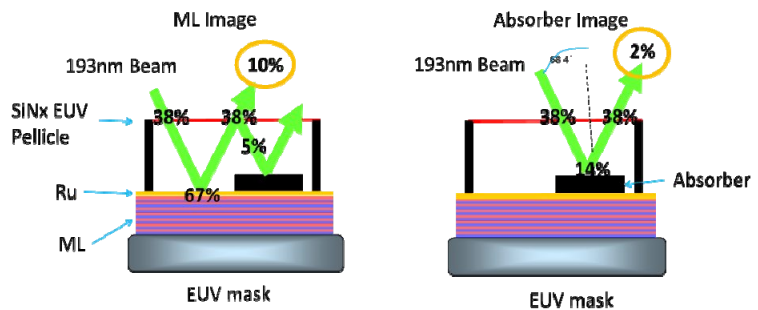


Figure 3: 193nm wavelength light collection

For the defect inspection tool, the low transmission means increasing the incident power to reduce imaging noise as much as possible (shot noise and sensor related noise). Further, there is the potential of imaging noise from the reflection from the inner surface of the pellicle. Finally, there is the potential for image quality degradation from variation in transmission versus incident angle.

4. TEST EUV MASK WITH EUV PELLICLE

To conduct this inspection experiment, we obtained an EUV mask which contained various line/space and hole patterns with programmed defects as shown in Figure 4. For this mask, the upper half and lower half of the reticle are identical. We then mounted a pellicle on the lower half to allow inspection experiments with and without the pellicle.

The EUV test reticle contains 1:1 horizontal and vertical line/space patterns from 36nm to 56nm pitch at 1x wafer dimensions (the actual patterns on the reticle are 4x). The hole patterns are both square and rectangular from 21nm to 42nm. There are a variety of programmed defect types in various sizes.

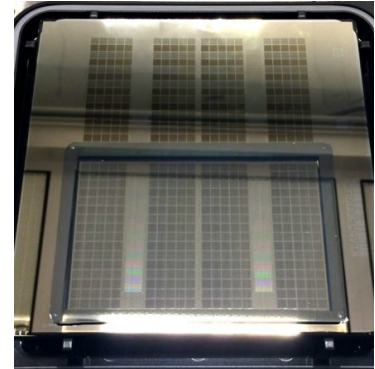


Figure 4: Actual EUV test mask with EUV pellicle covering lower half

5. PHOTOMASK INSPECTION BASICS

The diagrams in Figures 5 and 6 show the basic operation of photomask inspection consisting of Image Acquisition followed by Image Processing [2,3]. For basic illustration, this example is for transmitted light inspection of an optical reticle since it is easier to describe; the reflected light EUV mask inspection case is analogous.

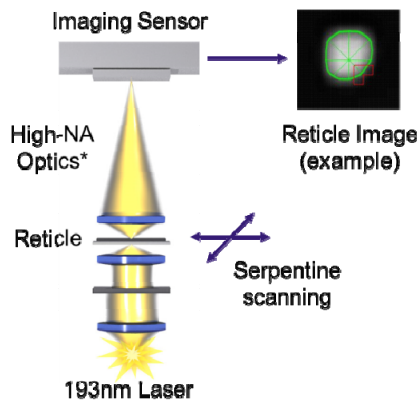


Figure 5: Mask inspection tool image acquisition (transmitted light case shown)

As shown, the surface of the mask is projected onto an imaging sensor using the high-NA optics. While an advanced 193nm wavelength wafer scanner has 1.35NA imaging at the wafer, it is 0.34NA at the mask due to the 4x reduction. To detect small defects on the mask, the defect inspection tool has more than 2x the NA of the scanner at the mask. Returning to Figure 5, the mask is mounted on an X-Y stage which moves it under the 193nm optics in a serpentine scan.

An example of a high-resolution image of a mask geometry is shown to the right in Figure 5. In this case, it is a transmitted light image of a hole. As the reticle is scanned, the image acquisition system outputs a steady stream of images from the reticle surface. The high-speed image stream is analyzed using custom high-speed image processing algorithms executing in a supercomputer.

Referring to Figure 6, a typical multi-die mask is shown; in this case, there are six identical die. Random defects such as fall-on particles or haze can be readily detected by comparing the

Referring to Figure 5, the inspection tool uses a 193nm wavelength laser for illumination (bottom of figure). For the KLA-Tencor tool, it is a high rep-rate solid state laser followed by special beam conditioning to smooth the pulses; this provides a continuous wave effect at the mask. Continuous wave is an advantage for the pellicle since the peak power density is lower versus inspection tools without pulse smoothing. The diagram shows the transmitted light illuminator below the mask and the high-NA imaging optics above the mask; there is also a reflected light path and illuminator which are not shown.

As shown, the surface of the mask is projected onto an imaging sensor using the high-NA optics. While an advanced 193nm wavelength wafer scanner has 1.35NA imaging at the wafer, it is 0.34NA at the mask due to the 4x reduction. To detect small defects on the mask, the defect inspection tool has more than 2x the NA of the scanner at the mask. Returning to Figure 5, the mask is mounted on an X-Y stage which moves it under the 193nm optics in a serpentine scan.

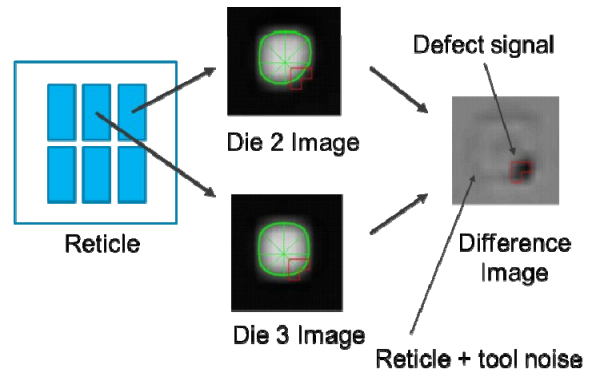


Figure 6: Mask inspection tool image processing (optical mask case shown)

images from two of the die, and then flagging anything that is different. In this case, during image processing, the geometry from die 2 is overlaid with the identical geometry from die 3 and any significant differences are flagged. For illustration, the lower left corners of the holes don't match which is then flagged as a defect. Notice in the difference image that there are some subtle differences in the rest of the hole. This is the result of subtle errors on the reticle and subtle errors in the inspection tool which are collectively referred to as "noise". The defect detection threshold is set to ignore these subtle differences while detecting the larger differences. Clearly, if the pellicle increases the "noise", then the detection threshold will need to be raised, thereby reducing defect detection sensitivity.

6. TEST RESULTS

6.1 Risks being assessed

Table 1 first lists the risks to the EUV pellicle itself of inspecting it with a 193nm wavelength defect inspection tool (lines 1, 2, and 3). The table then lists the risks to inspection tool performance of inspecting through this EUV pellicle versus no pellicle (lines 4, 5, and 6).

Lines 1 and 2 are the risk of breakage due to handling and/or stage acceleration. Further, the pellicle can shatter, so if it does break, there is risk of contaminating the inspection tool with particles thereby requiring cleaning. Line 3 is the risk that 193nm wavelength illumination may degrade the pellicle in some way which could impact wafer printing.

Line 4 is the impact of transmission vs. incident angle, which may cause image distortion and negatively impact defect sensitivity. Line 5 is the risk of the underside reflection which may also cause imaging noise and further impact defect sensitivity. Finally, line 6 is the low transmission of the pellicle which may cause imaging noise impacting sensitivity. Alternatively, low transmission may require slower inspection to improve SNR to retain good defect sensitivity.

Table 1: Pellicle and inspection risks being evaluated

	Parameter	Pellicle Risk	Inspection Risk	User Impact
1	reticle handling	breakage	n/a	tool damage
2	stage acceleration	breakage	n/a	tool damage
3	laser power	degradation	n/a	wafer impact
4	incident angle	n/a	image distortion	defect sensitivity
5	underside reflection	n/a	imaging noise	defect sensitivity
6	low transmission	n/a	imaging noise	defect sensitivity throughput

6.2 Pellicle durability initial test

We did some initial off-line tests of pellicle durability before loading the mask with pellicle into the inspection tool. Using a mask handling fixture, we did not observe any visual impact to the pellicle during normal automatic mask handling consisting of unloading from a pod, coarse alignment, then loading to a pod. Using a 193nm wavelength exposure fixture, we illuminated the pellicle with the power density used during inspection and didn't visually see any degradation. We then loaded the test reticle into the inspection tool for actual inspections and didn't observe any impact to the pellicle from handling or scanning.

6.3 Imaging distortion – base pattern modulation

With the test reticle and attached pellicle loaded in the inspection tool, we increased the incident power to be close to maximum and observed sufficient power on the imaging sensor for basic inspection (lower than normal but still viable). We then performed normal die-to-die inspections of various parts of the mask, analyzed the collected images, and assessed the performance.

Figure 7 shows a typical image of the EUV reticle. We compared base pattern modulation with and without the pellicle to assess the impact of image distortion caused by the pellicle. In this test we operated the tool under normal conditions of speed and focus and assessed base pattern modulation for three half-pitches both with and without the pellicle. To detect defects, defect SNR is the most critical parameter; whereas, base pattern modulation is less important. Some amount of base pattern modulation is helpful for alignment so some degradation is tolerable through the pellicle. Figure 8 shows the base pattern modulation comparison with and without the pellicle; the horizontal axis contains the three half-pitches assessed, the vertical axis shows the base pattern modulation. We measured less than 20% loss in base pattern modulation when inspecting through the pellicle, which we judge as acceptable for reasonable defect inspection.

Note that we aren't imaging exactly the same spot on the reticle, but rather two different spots with the same intended geometry – this represents a minor error source.

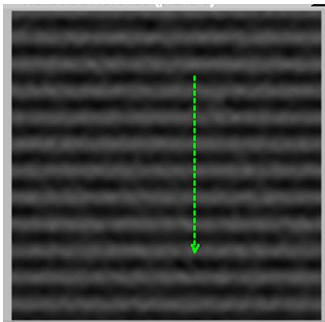


Figure 7: Typical reflected light image of EUV mask with inspection tool

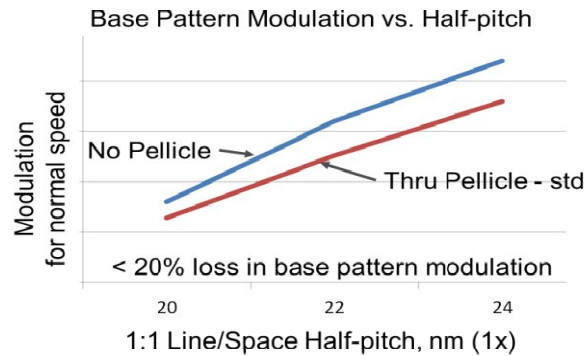


Figure 8: Base pattern modulation comparison without pellicle vs. with pellicle for different line/space half-pitches

6.4 Imaging distortion – defect signal

Since defect sensitivity is primarily impacted by defect signal, we then checked the modulation of selected defects with and without the pellicle. The difference image in Figure shows the signal of a typical defect; the magnitude of the bright spot (or dark spot).

The graph in Figure 10 shows the defect signal magnitude for two defect types in several small sizes: a dark extension and a pinhole. These defects were in an 18nm half-pitch line/space region (1x). The solid lines show the defect signal when there is no pellicle, whereas, the dotted line shows the signal through the pellicle. For both defect types the pellicle presents only a minor impact to defect signal considering the measurement errors.

Note that we aren't imaging exactly the same defects on the reticle, but rather two different defects with the same design – this represents a minor error source.

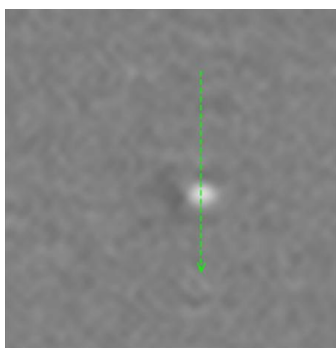


Figure 9: Typical defect signal in the inspection tool difference image

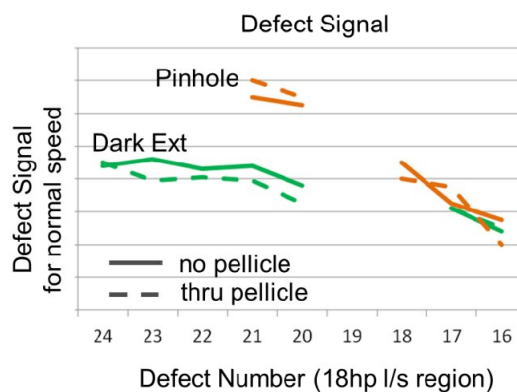


Figure 10: Defect signal comparison without pellicle vs. with pellicle

6.5 Through-pellicle 193nm inspection – initial test

We then did an actual die-to-die inspection through the pellicle in a region that was previously inspected before the pellicle was mounted. Figure 11 is a full area image of the EUV mask in the inspection tool as taken by its 1x camera. The green symbols overlaid on the image are the locations of the regions inspected. For this test, we inspected through the pellicle in the 32nm hole region, the 18hp horizontal line/space region, and the 18hp vertical line/space regions as shown. All regions contain programmed defects.

Figure 12 shows the defects detected for four defect types in the horizontal line/space pattern and four for the hole pattern with the defect designs shown to the far right. The defects are largest on the right and get progressively smaller going to the left. The blue bars show the defects detected before the pellicle was mounted (no pellicle case). The orange bars represent the defects detected through the pellicle. We didn't observe any defect sensitivity differences from the pellicle in the 32nm hole region, and only minor differences in the 18hp line/space region.

We did observe noticeable noise in some of the through pellicle difference images as shown in the small clip (mottling surrounding the defect). Based upon initial analysis of the images, we believe this is noise caused by the mask making process, but this needs further investigation. This noise complicated automated analysis, so we evaluated the defect signals manually.

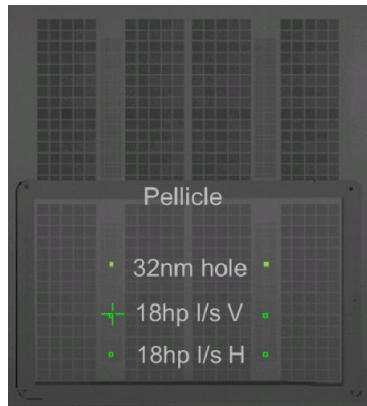


Figure 11: Image of EUV mask in inspection tool showing areas inspected

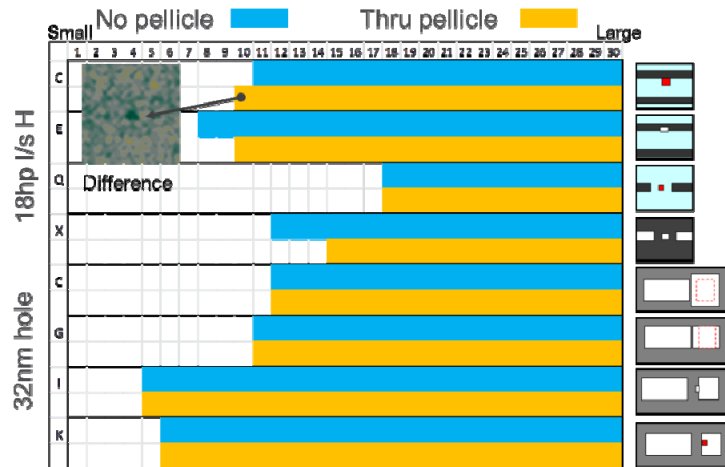


Figure 12: Inspection comparison without pellicle vs. with pellicle showing defects detected

7. CONCLUSIONS

In conclusion, then, we feel that the 19.6nm thick silicon-nitride EUV pellicle passed the initial 193nm inspection tests for durability, optical properties, and transmittance/reflectance.

In this initial test, we showed that standard 193nm inspection had good defect performance and that the optical properties of the pellicle had little negative impact.

8. POSSIBLE FUTURE WORK

From this initial work, we believe there are additional areas of study and possible improvement. These areas include: more extensive signal to noise ratio characterization with more patterns and defects, and more extensive characterization of signal-to-noise ratio versus throughput.

Further, we believe there is an opportunity to improve performance by developing optimum imaging for the through pellicle case.

Finally, we believe there may be sensitivity advantages to using slower throughput to increase light levels. In this way the user may be able to trade-off sensitivity versus throughput according to their use case.

However, before proceeding with further studies and experiments, we plan to assess the industry interest in this pellicle.

9. ACKNOWLEDGEMENTS

We thank the KLA-Tencor characterization and systems engineering teams for data collection and data analysis in support of this work. We are also thankful to Ravi Bonam from IBM as well as Jed Rankin and Karen Badger from Globalfoundries for technical support and useful discussions.

10. REFERENCES

- [1] D.L. Goldfarb, "Fabrication of a full-size EUV pellicle based on silicon nitride", *Proc. SPIE* 9635, 96350A (2015).
- [2] W.H. Broadbent, J.N. Wiley, Z.K. Saidin, S.G. Watson, D.S. Alles, L.S. Zurbrick and C.A. Mack, "Results from a new reticle defect inspection platform", *Proc. SPIE* 5256, 474 (2003).
- [3] W.H. Broadbent, J.N. Wiley, Z.K. Saidin, S.G. Watson, D.S. Alles, L.S. Zurbrick and C.A. Mack, "Results from a new die-to-database reticle inspection platform", *Proc. SPIE* 5446, 265(2004).